

CFD MODELLING OF CYCLONE SEPARATORS: VALIDATION AGAINST PLANT HYDRODYNAMIC PERFORMANCE

Matthew BRENNAN¹, Peter HOLTHAM¹, Mangadoddy NARASIMHA¹

¹The Julius Kruttschnitt Mineral Research Center, The University of Queensland, 40 Isles Rd, Indooroopilly, Queensland, 4068, AUSTRALIA

ABSTRACT

The major focus of CFD modelling of industrial process equipment is to simulate the industrial performance of the equipment with reasonable accuracy. In this paper results from CFD simulations of an industrial classification hydrocyclone and an industrial dense medium cyclone are compared with plant measurements from real cyclones of the same dimensions. The measurements used for validation are the feed pressure vs feed flow rate and recovery to underflow vs feed flow rate. The CFD simulations used Large Eddy Simulations, the Differential Reynolds Stress Model and laminar flow. On both cyclones, the DRSM and LES models gave considerably more accurate predictions compared to the laminar simulations and the DRSM model predictions were somewhat more accurate than predictions from the LES model.

NOMENCLATURE

$d_{63.2}$	slurry diameter at 63.2% of the size distribution - m
f_{kres}	ratio of resolved turbulent kinetic energy to total turbulent kinetic energy (see equation (4) in text)
g_i	gravity - $m.s^{-2}$
l_{sgs}	sgs filter length - m
p	pressure - kPa
r_f	fraction of feed reporting to underflow
t	time - s
u_{mi}	mixture velocity - $m.s^{-1}$
x_i	Cartesian dimension - m
C_s	Smagorinsky SGS constant
D_c	cyclone diameter - m
D_u	underflow diameter - m
D_{vi}	inner vortex finder diameter - m
D_{vo}	outer vortex finder diameter at tip - m
L_v	vortex finder length - m
H_c	length of cyclone cylinder - m
α_p	volume fraction of air
μ_{sgs}	sub grid scale eddy viscosity - $kg.m^{-1}.s^{-1}$
ρ_m	mixture density - $kg.m^{-3}$
τ_{ij}	stress tensor
θ	included angle of cyclone apex in degrees

INTRODUCTION

Cyclone separators are used extensively to classify mineral slurries with a size or density distribution in the mineral and coal industries. There are two variants, the classifying hydrocyclone which classifies on the size of the particle and the dense medium cyclone which classifies on particle density. The classifying hydro-

cyclone is used commonly to split the coarser tail fraction from the feed to a flotation cell for recycle to a mill. In dense medium separation, very fine ($d_{63.2} < 3.0 \times 10^{-5} m$) magnetite or ferro-silicon is added to the feed to increase apparent density of the fluid phase and the cyclone is used to partition larger particles about this apparent density. Dense medium cyclones are used mainly to separate coal from ash but are also used in iron-ore beneficiation.

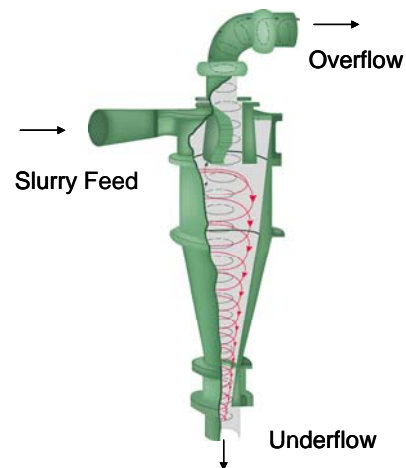


Figure 1, Typical cyclone shape showing inner and outer vortex structure

Both cyclone types have a similar shape. (shown in Figure 1) Internally the flow is a complex turbulent swirling multiphase flow with a free surface and a flow reversal. The slurry is fed tangentially into the upper cylindrical section through a nozzle which generates a forced vortex. An axial flow down the wall into the conical section occurs and a short distance from the underflow there is a flow reversal, where a proportion of the slurry turns radially inward to a free vortex which flows upward. The centrifugal force generated by this swirl has the effect of generating an axially aligned air core which is roughly cylindrical. More importantly, it is this centrifugal force, of the order 500g, which provides the classification force.

Dense medium cyclones are comparatively "short and fat" when compared to a classifying hydrocyclone because this shape reduces the residence time of the slurry and reduces medium segregation, which is detrimental to density partitioning.

There have been extensive studies where hydrocyclones have been modelled using Computational Fluid Dynamics (Narasimha et al 2007a). This CFD work has been validated by either Laser Doppler Anemometry (LDA)

conducted on a water flows in clear Perspex models (Hsieh 1998, Brennan 2006, Delgado 2006) or Gamma Ray Tomography measurements of density profiles in a plastic cyclone (Subramanian 2002, Narasimha et al , 2007b) or with an velocity probe (Brennan et al 2007b). Whilst both LDA, GRT and the velocity probe have generated useful data for validation, they are laboratory techniques which investigate the internal flow structure. LDA has been primarily been used on small cyclones. The velocity probe is an intrusive device. LDA, GRT and the velocity probe do not provide any information on how cyclones actually perform as industrial equipment.

There is a need to establish how well CFD modelling of hydrocyclones predicts the performance characteristics which are of interest to plant designers and operators such as the classification efficiency, the pressure drop vs flow behaviour and the recovery to underflow for particular cyclone designs. This has a number of interrelated aspects. Firstly there is need to establish how good the CFD predictions are across a range of cyclone geometries. Secondly there is a need to validate CFD predictions of the performance of large diameter cyclones, where industrial performance is the only data available. Finally it would also be useful to know the sensitivity of CFD predictions to small changes in the modelled shape. This is relevant because it has been the authors' experiences that there are often differences between nominal apparent measured dimensions due to manufacturing tolerances and different liners and this affects the CFD predictions.

In this paper the CFD predictions of hydrocyclones are compared to plant type measurement data rather than LDA. The measured data used for comparison is the pressure drop vs feed flow rate behaviour and the volumetric recovery to underflow, also as a function of feed flow rate. The work compares predictions from Large Eddy Simulation (LES) (Smagorinsky, 1963) and the differential Reynolds stress turbulence model (DRSM) (Lauder et al, 1975). The work looks at the predictions for two different cyclone designs and the work reports the sensitivity of predictions to small changes in the modelled cyclone shape for one particular design.

MODEL DESCRIPTION

Cyclone geometries and grid generation

Two geometries were chosen for the CFD study, which were a Krebs DF6 classifying hydrocyclone and a DSM pattern dense medium cyclone. Cyclones of these two geometries are available and the pressure drop and recovery to underflow as a function feed water flow rate was measured experimentally. The top view and elevations of the DF6 and DSM are shown in Figure 2 and the key dimensions are shown in Table 1. The DF6 cyclone is the typical long thin shape of a medium sized classifying cyclone with involute entry whereas the DSM is the typical short fat shape of a dense medium cyclone and has essentially tangential entry.

The grids were generated in Gambit and were 3 dimensional body fitted grids which encompassed the flow space from the feed port (at approximately the position of the feed pressure gauge) to the underflow and the top of the vortex finder. The approach used was identical to that reported by Brennan (2006), Brennan et al (2007a) and Narasimha et al (2007). The feed port was a

velocity inlet boundary condition (which was set up in the Fluent case using a fully developed turbulent flow profile (Bird et al, 1960)) and the overflow and underflow were pressure outlet boundary conditions. All other boundary conditions were wall boundaries. An extensive range of grids were generated for both cyclone geometries but only a subsection are reported here. The grids reported here are summarised in Table 2, which are a coarse and fine grid for the DF6 and the grid typically used for all DSM geometries. The LES on the DF6 coarse grid has been previously reported by Brennan et al (2007b).

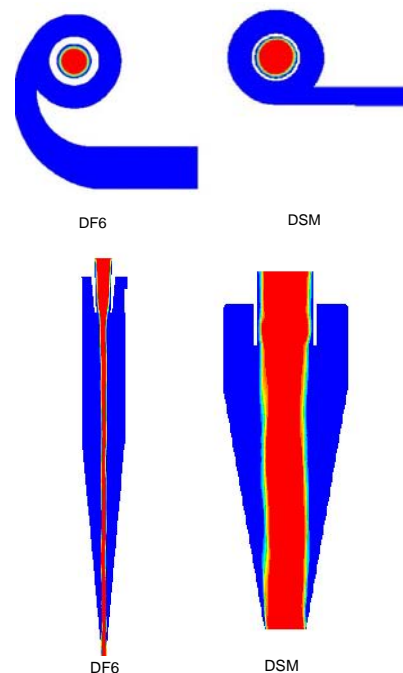


Figure 2 - Top view and elevations of the two cyclones used in study (not to scale)

Dimension	DF6	DSM
D_c - m	0.152	0.300
A_f - m ²	3.841×10^{-3}	7.335×10^{-3}
D_{vi} - m	0.050	0.129*
D_{vo} - m	0.063	0.150
L_v - m	0.1255	0.100
D_u - m	0.025	0.100
H_c - m	0.580	0.200
θ - deg	10	20

Table 1 - Key dimensions of cyclones used in study.

*Reference D_{vi} in DSM perturbation studies = 0.124 m

Grid points	DF6 -coarse	DF6 - fine	DSM*
Tangential	60	120	48
Radial	14	30	33
Axial in cylinder	54	96	28
Axial in apex	50	100	50
Volume elements	1.88×10^5	1.33×10^6	1.48×10^5

Table 2 - Summary of grids used in study. *For DSM: typical for all geometric perturbations

Investigations of small changes in cyclone shape were conducted using the DSM geometry. Here the cyclone diameter was kept fixed at 0.300 m but grids were generated where the A_i , D_{vi} , D_{vo} , L_v , D_u , H_c and θ were varied by a small amount from the dimensions of a reference geometry. This reference geometry had the same dimensions as given in Table 1 except that the inner vortex finder diameter D_{vi} was 0.124m.

CFD modelling

The CFD was solved in Fluent 6.3.26 using the VOF model (Hirt and Nichols, 1980) Here only one set of the equations of motion are solved in the domain (ie for the mixture):

$$\frac{\partial \rho_m}{\partial t} + \frac{\partial \rho_m u_{mi}}{\partial x_i} = 0 \quad (1)$$

$$\frac{\partial}{\partial t} (\rho_m u_{mi}) + \frac{\partial}{\partial x_j} (\rho_m u_{mi} u_{mj}) =$$

$$-\frac{\partial}{\partial x_i} p + \frac{\partial}{\partial x_j} (\tau_{\mu,ij} + \tau_{d,ij} + \tau_{t,ij}) + \rho_m g_i$$

The VOF model is intended for CFD problems where there is a free surface between two immiscible continuous fluid phases and was used to resolve the air core. The primary phase was treated as water and the secondary phase was treated as air. The VOF model solves a transport equation for the air phase concentration:

$$\frac{\partial}{\partial t} \alpha_p + \frac{\partial}{\partial x_i} (\alpha_p u_{mi}) = 0 \quad (3)$$

The turbulent stresses in the tensor $\tau_{i,j}$ were calculated using (a) the DRSM (Launder et al, 1975) with the Launder Linear pressure strain model and also (b) LES using the standard Smagorinsky-Lilly sub grid scale model with a default $C_s=0.1$ (Smagorinsky 1963). The DRSM simulations used standard wall functions. A simulation with laminar flow (ie no turbulence model) at rated flow was also conducted with each cyclone design.

The equations were solved using the unsteady segregated solver with a time step of 1×10^{-4} s. The following discretization options were used: SIMPLE for pressure-velocity coupling, PRESTO for pressure and QUICK for the VOF equation. The momentum equations used QUICK with the DRSM simulations and Bounded Central Differencing with LES. The numerical approach was to start with the cyclone domain “full of water” and at a base flow rate and integrate in time until the swirl created a axial region of negative pressure. At this point the backflow volume fraction of air at the overflow and underflow was set to 1 and the simulation proceeded so that air was drawn in to form the air core. The integration then proceeded until steady mass flow rates out the overflow and underflow and a steady feed pressure were obtained. This base case was used as an initial condition for cases at other flow rates. In the DSM simulations where small perturbations were made to the geometry, all cases were initialized using by interpolating the data from a converged case for the reference geometry. The DF6 cyclone was simulated in a vertical position and the DSM cyclone was simulated with the axis at 20° to the horizontal. The results reported here are at steady state, which was achieved after around 5s of simulation time.

RESULTS – COMPARISON BETWEEN GEOMETRIES

Predicted tangential velocities at rated flow

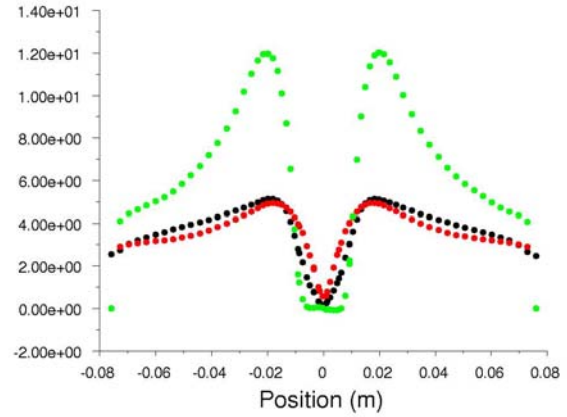


Figure 3 - Tangential velocities – $m.s^{-1}$, 0.350 m below top of cyclone. DF6 cyclone coarse grid at $4.9 kg.s^{-1}$. ● DRSM, ● LES (Mean), ● laminar solver

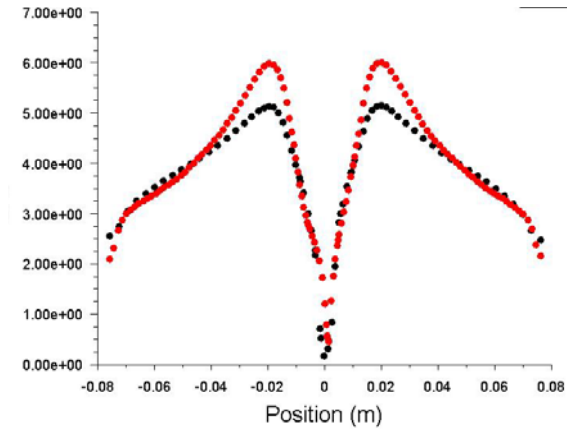


Figure 4 - Tangential velocities – $m.s^{-1}$, 0.350 m below top of cyclone. DF6 cyclone at $4.9 kg.s^{-1}$. ● LES fine grid (Mean), ● LES coarse grid (Mean)

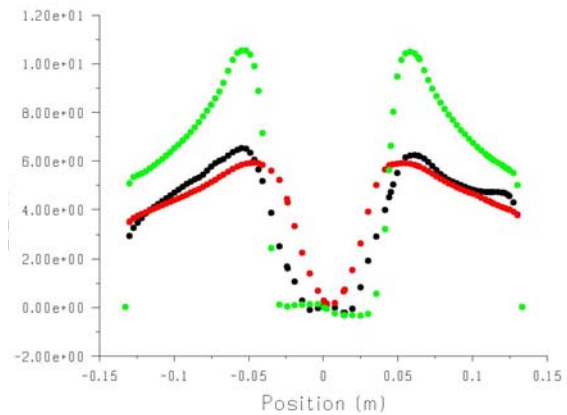


Figure 5 - Tangential velocities – $m.s^{-1}$, 0.300 m below top of cyclone. 0.300 m DSM cyclone at $12.2 kg.s^{-1}$. ● DRSM, ● LES (Mean), ● laminar solver

Cyclone separators operate normally at tangential velocities around $5-6 m.s^{-1}$, which is achieved at a feed

water flow rate around 4.9 kg.s^{-1} in the DF6 cyclone and, 12.2 kg.s^{-1} in the DSM design. The tangential velocities at these flow rates are shown in Figure 3 and Figure 4 for the DF6 and Figure 5 for the DSM. (Mean velocities are shown for the LES.) For both cyclone geometries the DRSM turbulence model predicts lower tangential velocities than the LES on the same grid. However velocity predictions with the laminar solver are around twice the velocity predictions from either LES or DRSM and when compared to the laminar predictions LES and DRSM predictions are similar. This would suggest that the LES is resolving some of the radial turbulent momentum transfer. However Figure 4 indicates that the LES predictions are not grid independent with the tangential velocity increasing by 20% with the finer grid.

Turbulence statistics were collected on both the fine and coarse grid LES for the DF6 and contours of the ratio of the resolved turbulent kinetic energy to the total turbulent kinetic energy calculated according to the equation:

$$f_{kres} = \frac{0.5u_i'u_i'}{0.5u_i'u_i' + (\mu_{sgs} / C_s l_{sgs} \rho_m)^2} \quad (4)$$

are shown in Figure 6. For a "good" LES, f_{kres} should be at least 0.9 and Figure 6 shows that this is not achieved in the DF6 coarse grid LES.

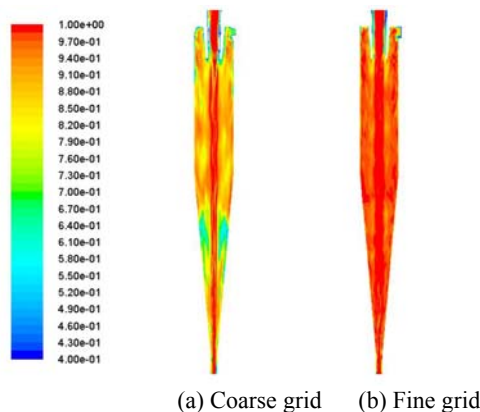


Figure 6 - Ratio of resolved turbulent kinetic energy to total turbulent energy for DF6 cyclone LES.

Predicted flow rate and recovery to underflow as a function of feed pressure

Water flow and pressure measurements were conducted on an industrial Krebs DF6 cyclone and a 0.300 m DSM geometry. The cyclones were fed from a sump via an electric pump with a facility to adjust the feed flow rate. A pressure gauge was located at the cyclone inlet. The feed flow rate was found from the sum of the overflow and underflow flow rates. On the DF6 cyclone, the flow rates could be measured with a 20l bucket, electric scales and a stop watch. The flow rates from the DSM cyclone were too large to measure directly and were passed through a Vezin sampler, which is a rotary device which diverts the flow to the bucket for only a fixed proportion of the rotation of the sampler. For the DSM cyclone the flow rates were calculated as the mass of water collected over a given time divided by the fraction of the flow diverted.

Comparisons between the measured feed water pressure and the measured fraction of feed water reporting to

underflow with LES and DRSM predictions are shown in Figure 7 to Figure 10. (The LES predictions on the DF6 are from the coarse grid.) These figures show that for both cyclone designs, the predicted feed pressure from the DRSM is consistently closer to the measured pressure than the pressure predicted from LES. The LES also predicts a higher pressure than the DRSM, which is consistent with the LES predicting higher tangential velocities.

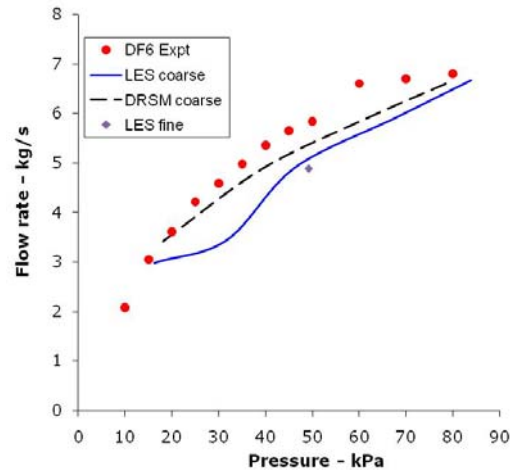


Figure 7 - Flow rate as a function of feed pressure for DF6 cyclone.

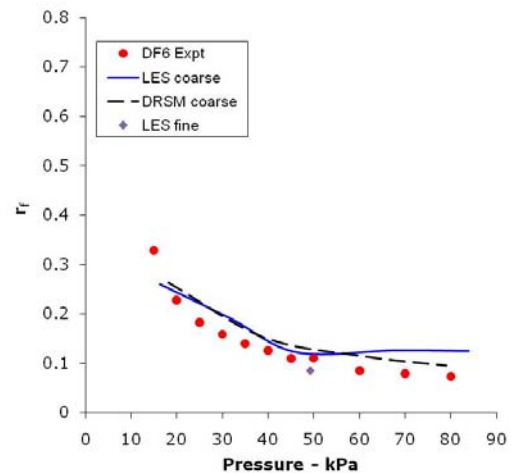


Figure 8 - Fraction of feed reporting to underflow as a function of feed pressure for DF6 cyclone.

Simulations with the laminar solver were only conducted at the nominal rated flow. For the DF6 cyclone at 4.89 kg.s^{-1} , laminar simulations predicted a feed pressure of 125 kPa and an r_f of 0.012, compared to 35 kPa and 0.15 for experiment. For the DSM cyclone at 12.2 kg.s^{-1} , laminar simulations predicted a feed pressure of 76.5 kPa and an r_f of 0.169, compared to 35 kPa and 0.3 for experiment. The feed pressures predicted by the laminar solver are considerably larger than measured feed pressures and the laminar predicted r_f is too low. This is an indication that the tangential velocities are excessively over-predicted by the laminar solver (Figure 3 and Figure 5) and that the predictions for both the DRSM and LES are comparatively much closer to experiment even though the DRSM predictions seem more accurate.

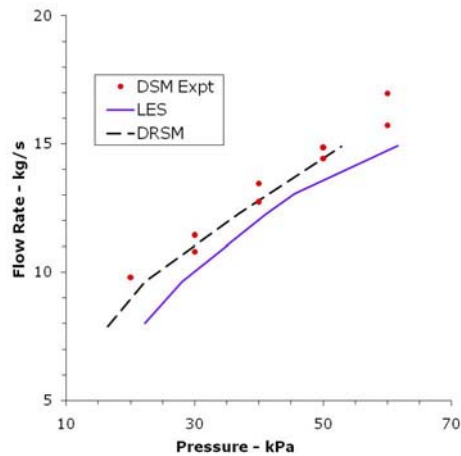


Figure 9 - Flow rate as a function of feed pressure for DSM cyclone

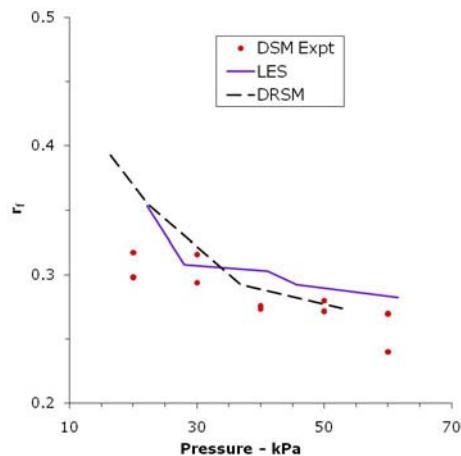


Figure 10 - Fraction of feed reporting to underflow as a function of feed pressure for DSM cyclone

A Fine grid LES on the DF6 was only run at the rated flow of 4.9 kg.s^{-1} . This simulation predicted a feed pressure of 49.2 kPa , which is actually poorer than the coarse grid LES prediction of 44.7 kPa , and predicted an r_f of 0.14 .

The pressure drop across any cyclone is the sum of the inlet nozzle pressure drop and the wall pressure near the top of the body, which is the radial integral of the centrifugal acceleration. The contours of predicted pressure for the DSM at a feed water flow rate of 12.2 kg.s^{-1} for both the LES and DRSM are shown in Figure 11 and indicate that the wall pressure is fairly constant in the upper section and for the LES is 32 kPa and for the DRSM is 27.5 kPa . For both simulations the pressure drop across the inlet nozzle is about 10 kPa and hence the difference between the feed pressure predicted by LES and DRSM on the DSM geometry (see Figure 9) is due mainly to the differences in the predicted tangential velocities.

The dimensions of both cyclones were double checked and it is considered doubtful that there were errors in the modeled geometries so it is felt that the DRSM model is predicting the tangential velocity more accurately in these simulations.

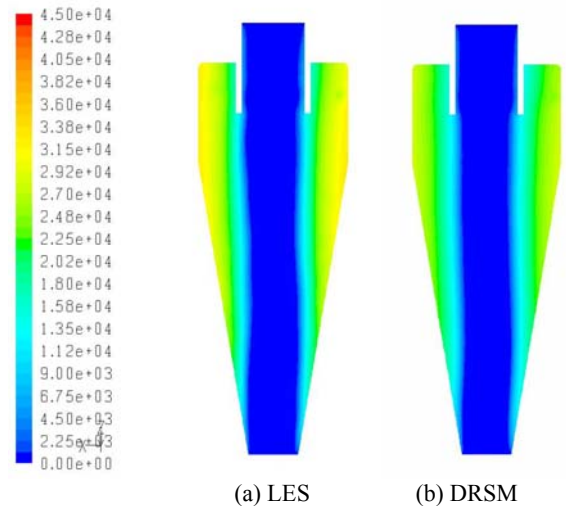


Figure 11 - Contours of pressure from (a) LES, (b) DRSM, on DSM cyclone at 12.2 kg.s^{-1} feed water flow rate

This conclusion is at variance from our earlier work (Brennan, 2006, Brennan et al 2007) where the LES model gave better tangential velocity predictions than the DRSM when compared to published LDA data of Hsieh (1988), though this work was conducted on a smaller 0.075 m cyclone. It is also apparent that refining the grid makes the DF6 LES predictions worse. This is because the SGS eddy viscosity, which is carrying a proportion of the shear stress is reduced from typically $0.06 \text{ kg.m}^{-1}.\text{s}^{-1}$ on the coarse grid to around $0.03 \text{ kg.m}^{-1}.\text{s}^{-1}$ on the fine, but the resolved Reynolds shear stresses remain largely unchanged and hence the predicted tangential velocity increases.

The implication is that the LES is predicting less turbulence than is occurring in reality. This may be because the grids used were too coarse for the LES model. This is problematic because the fine grid LES on the DF6 is only computationally practical for a two-phase water-air simulation. This may be less of a problem in multiphase simulations because the viscosity of slurries increases at high particle loadings ($\sim 0.03 \text{ kg.m}^{-1}.\text{s}^{-1}$), but this conclusion from this work is that the LES model should be used with care in CFD of larger cyclones and the DRSM model might be the better model.

In terms of modelling classification in hydrocyclones, either the DRSM or the LES can be used with the mixture model (Manninen et al 1996) as reported by Brennan et al (2007a). An attraction to LES is that it solves 6 less transport equations than the DRSM and passes a resolved instantaneous velocity to the slip velocity calculation compared to a Favre averaged velocity with the DRSM. Hence the LES should automatically simulate the turbulent mixing of the dispersed phases associated with the resolved fluctuations with the base mixture model. For turbulent mixing to be modelled in a DRSM simulation, the acceleration associated with the gradient of the Reynolds stresses needs to be included in the slip velocity calculation (see Manninen et al 1996). However this relative advantage of the LES is of no merit if a computationally impractical grid is needed to resolve the turbulence.

RESULTS – SMALL CHANGES IN DSM GEOMETRY

Simulations on grids where the DSM geometry was changed by a small amount were performed using the LES model at a feed water flow rate of 12.2 kg.s^{-1} . The feed pressure P_f and fraction of feed reporting to underflow were recorded once each simulation has reached steady flow. $P_f=42.5 \text{ kPa}$ and $r_f=0.33$ for the reference grid. The results from these simulations are summarised in Figure 12 for feed pressure and Figure 13 for fractional recovery to underflow. These graphs show that the feed pressure is quite sensitive to small changes in vortex finder shape, inlet port area A_i and underflow diameter D_u , but the sensitivity is not necessarily linear in change. For example if D_u is increased by 5%, P_{feed} is reduced by 3% but if D_u is decreased by 3%, P_{feed} goes up by only $\sim 1.5\%$. It is apparent however that r_f is sensitive to changes in D_u and the inner vortex finder diameter D_{vi} . These simulation results point out that cyclones need to be checked regularly for wear if cyclone performance is to be maintained.

The results also indicate that the simulated geometry has to be a close match to the actual geometry, i.e. within 5%. This is problematical where the only reference for the CFD simulation is the actual device since it is difficult, particularly in a plant environment, to measure the exact dimensions of real devices with precision.

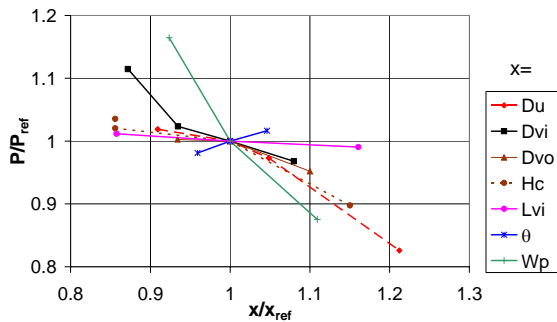


Figure 12 - Ratio of P_{feed} to $P_{\text{feed,ref}}$ for perturbations about reference DSM geometry

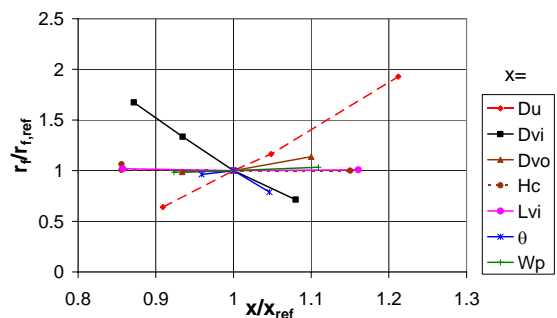


Figure 13 - Ratio of r_f to $r_{f,ref}$ for perturbations about reference DSM geometry

CONCLUSIONS AND RAMIFICATIONS FOR TURBULENCE MODELLING

A series of water/air CFD simulations of two industrial cyclone designs with diameters of 0.150 and 0.300 m have been conducted and predictions have been compared to

measurements of feed flow vs feed pressure and fraction of feed reporting to underflow vs feed pressure on real cyclones of the same geometry. The CFD predictions from the DRSM model are consistently in good agreement with the measurements, whereas the LES over predicts the feed pressure by around 5-10 kPa. The prediction of the fraction of feed reporting to underflow is also closer to measured with the DRSM model, though r_f predictions from both turbulence models are satisfactory.

This would therefore suggest that on these coarse grids, for these designs, for water flow, the DRSM model is the more satisfactory technique. However what happens at high feed solids concentrations, where the slurry viscosity is much larger than the viscosity of water and the flow less turbulent may be different and the choice of turbulence model here needs further investigation.

Simulations have been conducted using the 0.300 m DSM geometry where the simulated dimensions were adjusted by small amounts. The simulations give an indication of the sensitivity of the CFD to changes in geometry at this level and indicate that the dimensions of the simulated geometry need to be within 5% of the actual geometry.

REFERENCES

- BIRD, R. B., STEWERT, W. E., LIGHTFOOT, E. N. (1960), Transport phenomena, Wiley, New York, page 155.
- BRENNAN, M., (2006), CFD simulations of hydrocyclones with an air core – comparison between large eddy simulations and a second moment closure, *Chemical Engineering Research and Design*, 84A, 495-505.
- BRENNAN, M. S., NARASIMHA, M., HOLTHAM, P. N., (2007a), Multiphase modelling of hydrocyclones – prediction of cut-size, *Minerals Engineering*, 20, 395-406.
- Hsieh, K. T., (1988), A phenomenological model of the hydrocyclone, Ph D Thesis, University of Utah.
- BRENNAN, M. S., FRY, M., NARASIMHA, M., HOLTHAM P. N., (2007b), Water velocity measurements inside a hydrocyclone using an Aeroprobe & comparison with CFD predictions, 16th Australasian Fluid Mechanics Conference Crown Plaza, Gold Coast, Australia 2-7 December.
- DELGADILLO J., 2006, "Modelling of 75 and 250 mm hydrocyclones and exploration of novel designs using computational fluid dynamics", Ph D Thesis, University of Utah.
- FLUENT 6.3 Users Guide (2006), Lebanon, NH, USA.
- HSIEH, K. T., (1988), A phenomenological model of the hydrocyclone, Ph D Thesis, University of Utah.
- HIRT, C. W., NICHOLS, B. D., (1981), "Volume of fluid (VOF) method for the dynamics of free boundaries", *Journal of Computational Physics*, 39, 201-225.
- LAUNDER, B.E., REECE, G.J., RODI, W., (1975), "Progress in the development of a Reynolds-stress turbulence closure", *Journal of Fluid Mechanics*, 68, 537-566.
- MANNINEN, M., TAIVASSALO V., KALLIO S., (1996), "On the mixture model for multiphase flow", Valtion Teknillinen Tutkimuskeskus, Espoo, Finland.
- NARASIMHA M., BRENNAN M., HOLTHAM P. N., (2007a), "A review of CFD modelling for performance predictions of hydrocyclones", *Engineering Applications of Computational Fluid Dynamics*, 1, 71-87.
- NARASIMHA, M., BRENNAN, M. S., HOLTHAM, P. N., NAPIER-MUNN T. J., (2007b), "A comprehensive CFD model of dense medium cyclone performance", *Minerals Engineering*, 20, 414-426.
- SMAGORINSKY, J., (1963), "General Circulation Experiments with the Primitive Equations. I. The Basic Experiment.", *Month. Wea. Rev.*, 91, 99-164
- SUBRAMANIAN, V.J., (2002), "Measurement of medium segregation in the dense medium cyclone using gamma-ray tomography", Ph.D. Thesis, JKRC, University of Queensland.